Fluid drag-reducing effect and mechanism of superhydrophobic surface with micro-nano textures

Jingxian ZHANG [1], Zhaohui YAO [1,*], Pengfei HAO [1], Haiping TIAN [2], Nan JIANG [2]

* Corresponding author: Tel.: ++86 10 6277 2558; Email: yaozh@tsinghua.edu.cn
1: Department of Engineering Mechanics, Tsinghua University, P.R. China
2: School of Mechanical Engineering, Tianjin University, P.R. China

Abstract In this paper, drag-reducing property and mechanism of superhydrophobic surface are investigated. Superhydrophobic surfaces with micro-nano textures were fabricated and tested using SEM and contact angle measurement. Experiments on a channel and a flat plate with superhydrophobic surface were conducted separately. For the channel flow, the drag was acquired by measuring the pressure loss. A 54% drag reduction was found both in laminar and turbulent flow over Re range from 500 to 5000. For flow over a plate, PIV measurement was used to obtain the velocity distribution at Re_δ=12000. There was a 19% reduction on the total stress in the whole boundary layer. Suppressions of the turbulence intensities and the Reynolds shear stress were found, which may cause the drag reduction.

Keywords: Superhydrophobic surface, Micro-nano textures, Drag reduction, PIV

1. Introduction

Superhydrophobicity in nature has been known for some time. With superhydrophobic effect, lotus can remain clean in murky ponds and water striders can stand freely and move quickly on water surface.

Superhydrophobic surfaces can also be produced in the laboratory. Nishino et al. (1999) measured the free energy for the surface of regular aligned closest hexagonal packed -CF3 groups. This surface free energy is considered to be the lowest of any solid. However, the dynamic contact angle of water on the surface was only 119°. This means superhydrophobicity not only depends on the surface chemistry, but also the topography of the surfaces. Feng et al. (2002) found nano-textures on the micro papilla of the lotus leaf, and these micro-nano-textures were thought as the key point to get the excellent superhydrophobic properties. Therefore, micro-nano-textures combined with suitable surface chemistry can make wonderful superhydrophobic surfaces.

With the unique water-repellent properties, superhydrophobic surfaces can be employed to produce drag reduction in both laminar and turbulent flows (Rothstein et al., 2010). Ou et al. (2004) investigated the flow through a series of microchannels (depth 76μm<H<254μm, aspect ratio W/H =20, and length L=50mm) containing a superhydrophobic surface. Both groove and post geometries were investigated and pressure drop reductions up to 40% were reported. It found that the drag reduction was effected by the pattern and size of the microstructure on the superhydrophobic surface. Choi et al. (2006) fabricated superhydrophobic surfaces by nano column structures with 500 nm high and 230 nm spacing. The superhydrophobic surfaces were applied to the 3 μm microtube. The pressure drop in it can be reduced by 20% ~ 30% than that in ordinary microtube. In the author's earlier studies (Lu et al., 2010), the superhydrophobic surfaces were used in the flow resistance experiment, with micro-nano composite structures and fabricated by winding carbon nanotubes. Comparing with the single-level structure, hierarchical structures had better drag-reducing effect for laminar flow.

Recently some researches on the turbulent flow drag reduction by superhydrophobic surfaces have been done.

Krupenkin et al. (2004) used superhydrophobic surfaces with two types of structures (nano grass and micro brick) to do the experiment. They found the drag reduction in turbulent flow was more apparent than that in laminar flow. Significant drag reduction has been measured by PIV and direct pressure measurements in turbulent flow over superhydrophobic microridge surfaces in the research of Daniello et al. (2009). In their study, no significant drag reduction or slip velocities were noted in the laminar regime. The onset of drag reduction occurs at a critical Reynolds number where the viscous sublayer thickness approaches the scale of the superhydrophobic microfeatures. Woolford et al. (2009) used the photolithography technology to fabricate the structured microribs and microcavities on the silicon wafers. Both longitudinal and transverse rib/cavity orientations were considered and the surfaces were made superhydrophobic by application of a Teflon coating. They found that the superhydrophobic surfaces exhibiting the longitudinal rib/cavity configuration were shown to yield an 11% decrease in the friction factor while the same surfaces exhibiting the transverse rib/cavity configuration were shown to cause a modest increase in the friction factor. Koji Fukagata et al. (2006) put forward a theoretical formula to calculate the turbulent drag reduction caused by the superhydrophobic surface. Similar researches have been done by the author's laboratory (Zhang et al., 2013). The superhydrophobic surface was fabricated by sticking micro-nano particles onto an aluminum or PMMA substrate. Compared with the common surface channel, the flow resistance decreases approaching 22.8% in the laminar flow. In the turbulent flow, the drag reduction can reach to 53.3%.

Some researches on external flow have been done. Gogte et al. (2005) applied superhydrophobic coating with micro textures to the surface of a hydrofoil, and observed a 10% or higher drag reduction in an external flow. Bixler and Bhushan (2013) conducted some experiments in an open channel with shark-skin riblet inspired microstructured surfaces. Experimental results indicate that the micro-textured surfaces effectively reduce Drag in open channel flow. Aljallis et al. (2013) observed obvious drag reduction in turbulent flow over an aluminum plate with superhydrophobic coating. They believed that the drag reduction is not only depends on the slip velocity, but also related to the morphology and stability of the surface air layer.

In this paper, superhydrophobic surfaces with micro-nano hierarchical textures were measured in channel flow and external flow. Following the details of the devised experimental methods and procedures, the measured results are reported. With these results, a significant drag-reducing effect of superhydrophobic surfaces was observed, and the mechanism of this effect is discussed.

2. Experimental methodology

2.1. Superhydrophobic surface preparation

In the experiment, superhydrophobic surfaces were prepared using a spray coating method. The coatings were made using a three-step method. First, dirt and debris must be removed from substrates to be coated, using ethanol, acetone and pure water. Then a binder layer based on hexone and butyl acetate (from Ross Nanotechnology Company) was sprayed on the substrates. Finally, hydrophobic nano-particles (from Ross Nanotechnology Company) dispersed in acetone were sprayed on the binder layer, and formed dispersed micro clusters which are similar to the micro papillae of a lotus leaf. The morphology of the surface with superhydrophobic coating was examined by scanning electron microscope (SEM), shown in Fig.1.

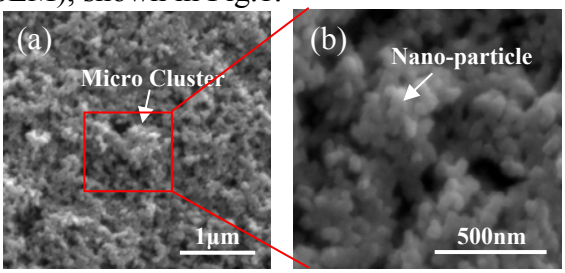

Fig. 1. Scanning electron microscope (SEM) images of the superhydrophobic coating. The arrow in (a)

indicates a micro cluster, whose details are shown in (b).

Contact angle meter (JC2000CD1) was used to measure the surface properties. The contact angle was measured as 161° and the rolling angle lower than 1° for a 10μL water droplet.

2.2. Experiments for drag measurement

A channel and a flat plate were prepared for the following experiment, with superhydrophobic coating sprayed on the measured surface.

2.2.1. Experiment for flow in the channel

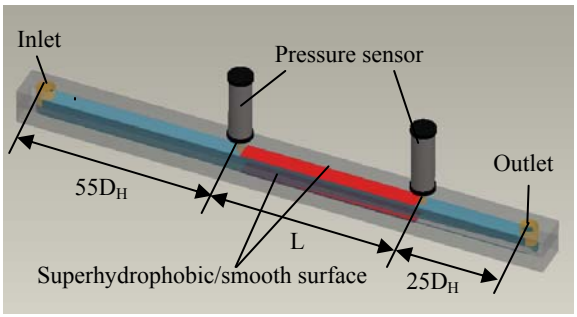

Fig. 2. Schematic of the channel used in the experiment

The channel used in the experiment was shown in Fig. 2. The length of the channel was 450mm, the transverse width of the channel was 9mm and the height of the channel was nominally 1.75mm, giving a hydraulic diameter, $D_H = 4A/P$, of 2.93 mm and a channel aspect ratio of nominally 0.194. A is the cross-sectional area and P is the cross-sectional perimeter. The middle part of the channel (shown in red color in Fig. 2) was replaceable that the experiments with the smooth surface and the superhydrophobic surface could be constructed in the same channel. Two pressure sensors were fixed at 55 D_H from the inlet and 25 D_H from the outlet respectively, to ensure the flow in the measured zone is fully developed.

An experimental apparatus was built to measure the pressure loss Δp along the channel under different Reynolds number, illustrated in Fig.3. An adjustable micro-bump was used to control the Reynolds number by adjusting the rate of flow. The mass flowrate Q_m was measured by a precise electrical balance.

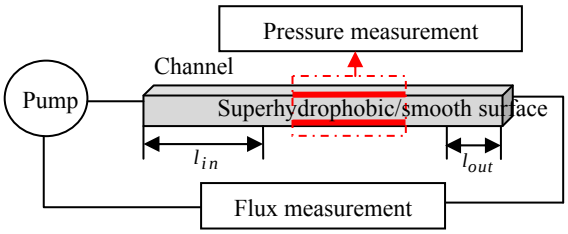

Fig. 3. Schematic of the experiment for flow in the channel (measuring zone with the superhydrophobic surface is marked by a red dotted line box).

The friction factor f in the channel can be calculated using the measured pressure loss Δp and the mass flowrate Q_m. It can be calculated as (Darcy-Weisbach formula):

$$f = \frac{\Delta p}{(L/D_H)} \frac{1}{\frac{1}{2}\rho U^2} \tag{1}$$

$$U = \frac{Q_m}{\rho A} \tag{2}$$

where L is the distance between the two measuring points, A is the cross-sectional area .

There are some empirical formulas for the friction factor f in a rectangular channel (Blevins, 1984).

For laminar flow (Re<2000), the friction factor is calculated as follows:

$$f = \frac{k}{\mathrm{Re}} \tag{3}$$

$$\mathrm{Re} = \rho U D_H / \mu \tag{4}$$

k is the dimensionless friction coefficient, which can be calculated as

$$k = \frac{64}{\frac{2}{3} + \frac{11}{24} r(2-r)} \tag{5}$$

In which r is the cross-sectional aspect ratio. In the experiment, k is 77.3.

For turbulent flow (Re>4000), the friction factor is calculated as follows:

$$f \approx \frac{0.316}{\mathrm{Re}^{0.25}} \tag{6}$$

In the paper, friction factors are obtained by experimental measurements and empirical

formulas. Then the flow drag in the common channel and superhydrophobic surface channel can be compared.

2.2.2. Experiment for flow over the plate

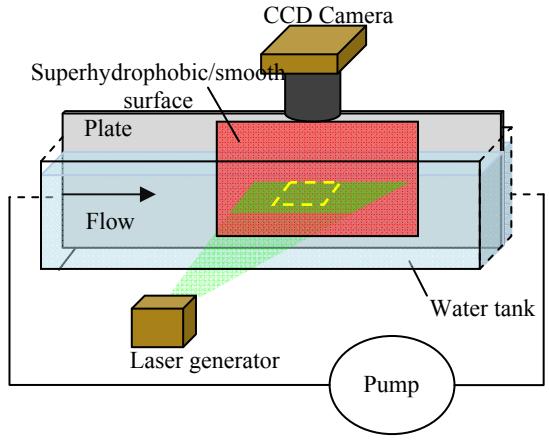

Fig. 4. Schematic of the experiment for flow over the flat plate

As shown in Fig. 4, the investigation was conducted in a water tank (5320 mm long, 250 mm wide and 380 mm deep). A plate was settled vertical in the water tank, and kept parallel to the sidewall of the water tank. The full length of the plate was 2400mm, and shown in the Fig. 4 is just its test part. The transverse width of the plate was 390mm. A tripping wire with diameter of about 10mm was settled at the leading edge of the plate, used to fix the boundary layer transition. The red zone on the plate shown in Fig.4 can be replaced by the superhydrophobic surface and the common surface. It was settled 1720mm away from the beginning of the plate, where the turbulent flow is considered fully developed. A layer of air is trapped on the superhydrophobic surface as soon as it merged in the water, and it could be observed by the different refletivity. The air layer exists during the whole experiment.

Particle image velocimetry (PIV) technology was used to measure the velocity field over the superhydrophobic surface. The flow field was seeded with 20 μm Polyamid particles. A Nd:YLF diode pumped laser was fixed in front of the water tank. The flow field in the test streamwise plane was illuminated by the laser light sheet, and then captured by the CCD camera (NanoSense, 1280×1024 pixels, 12 bit) at frame rates up to 500 fps. Each pixel corresponded to approximately 0.07mm. The interrogation spots were set to 32×32 pixels (streamwise × wall-normal direction). Each interrogation spot was overlapped by 75%, producing approximately 18000 vectors over a 95mm × 76mm field. Velocity fields could be obtained by cross-correlation method. Turbulent statistics were achieved by these velocity fields, including the normalized streamwise velocity $U=\overline{u}/U_\infty$, the turbulence intensity $U_{rms}=\sqrt{\overline{u'^2}}/U_\infty$ and $V_{rms}=\sqrt{\overline{v'^2}}/U_\infty$, and the Reynolds shear stress $T_{turb}=-\overline{u'v'}/U_\infty{}^2$.

The total shear stress T can be calculated as

$$T=\nu\frac{d\overline{u}/dy}{U_\infty{}^2}-\frac{\overline{u'v'}}{U_\infty{}^2} \quad (7)$$

where the bar on the parameter means the time-averged value of the parameter, such as $\overline{u}$ is the time-mean velocity for 6000 images. U_∞ is the mean velocity in free stream. u' and v' are the fluctuation velocities.

3. Result and discussion

3.1. Experiment for flow in the channel

The pressure drops in the channel under different Reynolds number were obtained. During the experiment, measurements for the smooth surface and the superhydrophobic surface are under the same control conditions.

Shown in Fig. 5 are profiles of the friction factor f as a function of Re for smooth and superhydrophobic surfaces. The friction factor f is calculated by Eq. (1), using the measured pressure values.

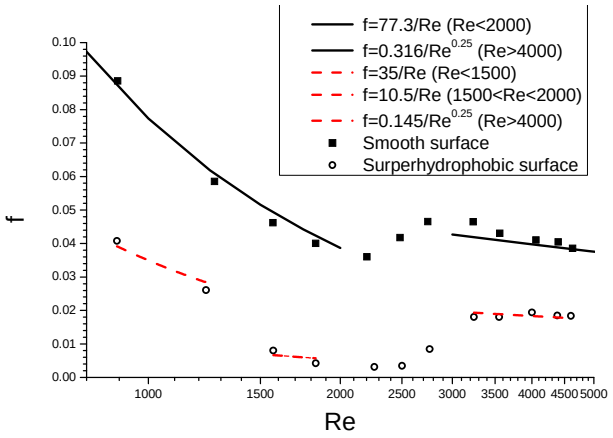

Fig. 5. Friction factor f as a function of Re for smooth and superhydrophobic surfaces

As shown in Fig. 5, the black solid lines represent the theoretical values calculated by empirical formulas for laminar flow (Eq. (3)) and turbulent flow (Eq. (6)). The square point and the circle point represent the data of the smooth and the superhydrophobic surface, respectively. The red dash lines are the fitting curves of the superhydrophobic surface.

For the smooth surface configuration, the f data shows a good agreement with the theoretical values both in laminar and turbulent flow.

For the superhydrophobic surface configuration, the friction factor f is much lower than that of the smooth surface in the whole Re range, which means significant drag reduction. This reduction can be expressed by the relative decrease in f, which can be calculated by comparing the fitting curves with the theoretical curves. In laminar flow (Re<2000), the form of the fit to the f data cannot be uniform. A sudden decrease in f occurs at Re=1500. At Re<1500, the form of the fit is $f = 35/\mathrm{Re}$, and the difference between this fit and the empirical formula shows a 54% reduction in f. At Re>1500, the form is $f = 10.5/\mathrm{Re}$, corresponding to an 86.4% drag reduction. In transitional flow (2000<Re<3000), a lager decrease in f of 88.2% is observed. This indicates that the drag-reducing effect of superhydrophobic surface is more evident in transitional flow, and it occurs at a critical Reynolds number of 1500. This phenomenon will be investigated in the future experiments. In turbulent flow (Re>3000), the reduction appears to be uniform, which is 54% in the entire turbulent range.

3.2. Experiment for flow over the plate

In the experiment, velocity fields for flow over the smooth and the superhydrophobic surface at Re_δ = 12000 (Re_δ is the Reynolds number of the boundary layer) are obtained, using the PIV method. 6000 instantaneous velocity fields were derived from two-frame cross-correlation, with 2ms time interval. With these instantaneous velocity fields, turbulent statistics illustrated in section 2.2.2 can be calculated.

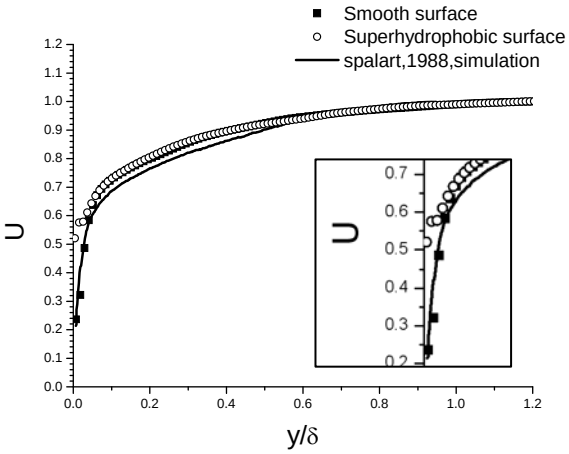

Fig. 6. Normalized mean velocity U, Re_δ=12000

Shown in Fig. 6 are profiles of the normalized time-averaged velocity U as a function of the normalized wall-normal coordinate y/δ (δ is the boundary layer thickness) at Re_δ =12000 (Re_θ=1140) for the smooth and the superhydrophobic surface conditions. The DNS result of Spalart(1988) at Re_θ=1410 is shown, too. In the earlier study (Spalart, 1988), it is reported that for Re_θ equal to 670 and larger (fully turbulent flow), the mean velocity profiles will be close to each other, which is reconfirmed in our experiment.

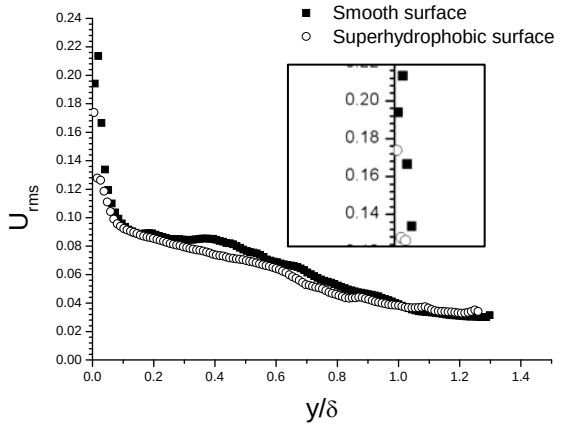

Fig. 7. Streamwise rms velocity U_{rms}, Re_δ =12000

Fig. 7 shows the normalized streamwise rms velocity U_{rms}, as a function of the normalized wall-normal coordinate y/δ. The curves for the two kinds of surface all decline as y/δ increases. For the superhydrophobic surface, slight suppressions of U_{rms} are found at the region of y/δ<0.8. At the near-wall region(y/δ<0.1), the U_{rms} of the superhydrophobic surface is much lower than that of the smooth surface, with a 17.2% reduction of the maximum value. The total reduction in the whole boundary layer (0 <y/δ<1) is 8%.

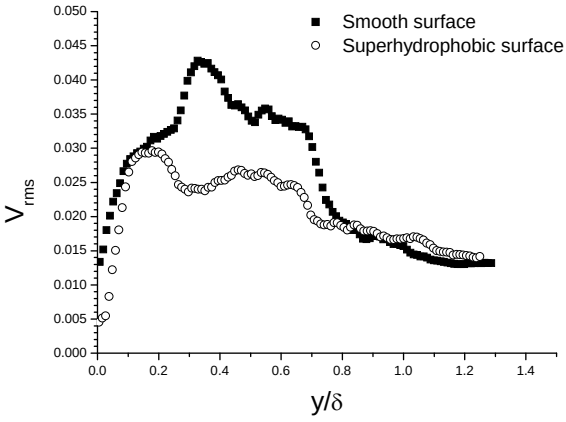

Fig. 8. Wall-normal rms velocity V_{rms}, Re_δ =12000

Fig. 8 shows the normalized wall-normal rms velocity V_{rms}, as a function of the normalized wall-normal coordinate y/δ. Similarly, suppressions of V_{rms} for superhydrophobic surface are found at the region of y/δ<0.8. The reduction of the maximum V_{rms} is about 30.5%, occurs at the region of y/δ<0.8. A 22.4% reduction is found in the whole boundary layer, which is more evident than the decrease in U_{rms}.

Shown in Figure 9 are profiles of the Reynolds shear stress T_{turb} (top panel) and the total shear stress T (bottom panel) as a function of the normalized wall-normal coordinate y/δ at Re_δ =12000. For the smooth surface, both the T_{turb} and T have a typical behavior of fully developed turbulent boundary flow. The Reynolds shear stress T_{turb} increases from 0 to the maximum value (about 0.00045) at the near-wall region(y/δ<0.1), and remains almost the same until y/δ=0.25. Then the T_{turb} declines slowly, and close to 0 near the top of the boundary layer. Different from the Reynolds shear stress T_{turb}, the total shear stress T has a constant value at wall, due to the viscous stress. Then the T rapidly increases to the maximum value 0.00153 at y/δ=0.03 and decreases to 0.00054 at y/δ=0.1. At y/δ>0.1, the total stress T has a similar behavior with T_{turb}.

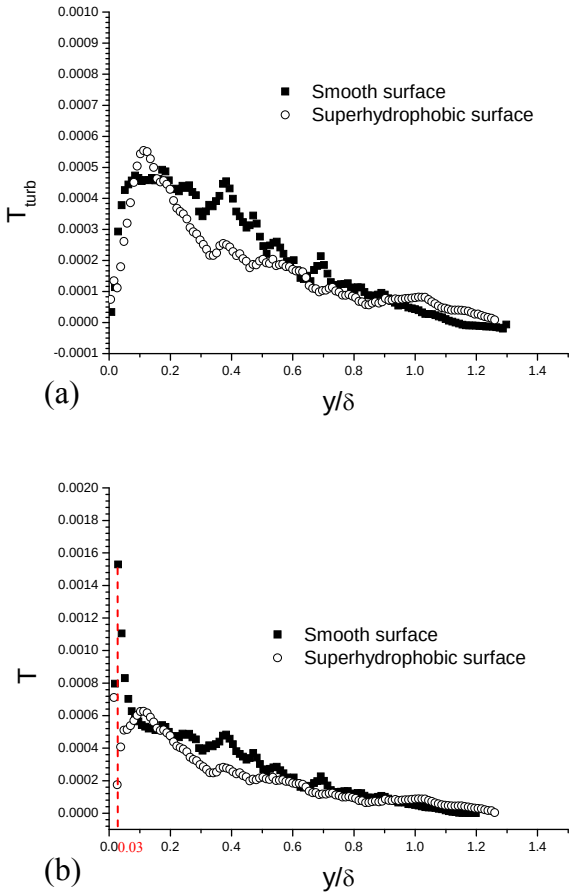

Fig. 9. (a) Reynolds shear stress T_{turb}, Re_δ =12000; (b)Total shear stress T, Re_δ =12000

At the region of $y/\delta<0.1$ and $0.2<y/\delta<0.8$, for both the T_{turb} and T, curves of the superhydrophobic surface are lower than those of the smooth one. The T_{turb} has a 28.3% reduction in range of $0.2<y/\delta<0.8$, and a 7.1% reduction in the whole boundary layer. The total shear stress T has a 19% reduction in the whole boundary layer, and the maximum value of T reduces 53.5%. At the region of $0.1<y/\delta<0.2$, slight increases in the T_{turb} and T for the superhydrophobic surface are observed, which will be investigated in the future.

4. Conclusions

In the paper, superhydrophobic surfaces with micro-nano textures were fabricated, using the spray coating method. Two experimental apparatus were designed and constructed to research the flow in the channel and over the flat plate with superhydrophobic surfaces. Significant drag reductions were found both in channel and plate case with superhydrophobic surfaces.

For channel flow, pressure measurement was used to quantize the flow resistance over the Reynolds number range from 500 to 5000. More than 54% reduction of the friction factor was found for channel with superhydrophobic surfaces, both in laminar and turbulent flow. The reduction in transitional flow was even 88.6%.

For flow over the plate, PIV technology was used to obtain the velocity field distribution. The Reynolds number of the boundary layer Re_δ is 12000. Reductions were found in the turbulence intensities U_{rms}, V_{rms}, Reynolds shear stress T_{turb} and total shear stress T, by comparing their distributions of the smooth surface case and the superhydrophobic surface case. This suggests that the superhydrophobic surface can suppress the turbulence fluctuation near the wall in the transition region. A reduction overall the turbulent boundary layer in the total stress T of 19% was found.

Acknowledgments

This work is supported by Grants-in-Aid from the National Natural Science Foundation of China (No. 11272176).

Reference

Aljallis, E., Sarshar, M. A., Datla, R., Sikka, V., Jones, A., & Choi, C. H., 2013. Experimental study of skin friction drag reduction on superhydrophobic flat plates in high Reynolds number boundary layer flow. Physics of Fluids (1994-present), 25(2), 025103.

Bhushan, B., Jung, Y. C., 2006. Micro-and nanoscale characterization of hydrophobic and hydrophilic leaf surfaces. Nanotechnology, 17(11), 2758.

Bixler, G. D., Bhushan, B. , 2013. Fluid Drag Reduction with Shark‐Skin Riblet Inspired Microstructured Surfaces. Advanced Functional Materials,23(36), 4507-4528.

Blevins, R. D., 1984. Applied fluid dynamics handbook. New York, Van Nostrand Reinhold Co., 1984, 568 p., 1.

Chen, W., Fadeev, A. Y., Hsieh, M. C., Öner, D., Youngblood, J., McCarthy, T. J., 1999. Ultrahydrophobic and ultralyophobic surfaces: some comments and examples. Langmuir, 15(10), 3395-3399.

Choi, C.H., Ulmanella, U., Kim, J., Ho, C.M., Kim, C.J., 2006. Effective slip and friction reduction in nanograted superhydrophobic microchannels. Physics of fluids, 18: 087105.

Daniello, R.J., Waterhouse, N.E., Rothstein, J.P., 2009. Drag reduction in turbulent flows over superhydrophobic surfaces. Physics of Fluids, 21 (1-9): 085103.

Davies, J., Maynes, D., Webb, B. W., & Woolford, B, 2006. Laminar flow in a microchannel with superhydrophobic walls exhibiting transverse ribs. Physics of Fluids (1994-present), 18(8), 087110.

Feng, L., Li, S.H., Li, Y.S., Li, H.J., Zhang, L.J., Zhai, J., Song, Y.L., Liu, B.Q., Jiang, L., Zhu, D.B., 2002. Super-hydrophobic surfaces: From natural to artificial. Advanced Materials, 14(24), 1857-1860.

Fukagata, K., Kasagi, N., Koumoutsakos, P., 2006, A theoretical prediction of friction drag reduction in turbulent flow by superhydrophobic surfaces. Physics of Fluids (1994-present), 18(5): 051703.

Gogte, S., Vorobieff, P., Truesdell, R., Mammoli, A., van Swol, F., Shah, P., & Brinker, C. J., 2005. Effective slip on textured superhydrophobic surfaces.Physics of fluids, 17(5), 51701-51701.

Krupenkin, T.N., Taylor, J.A., Schneider, T.M., et al., 2004. From rolling ball to complete wetting: the dynamic turning of liquids on nanostructured surfaces. Langmuir, 20(10): 3824-3827.

Nishino, T., Meguro, M., Nakamae, K., et al., 1999. The Lowest Surface Free Energy Based on $-CF_3$ Alignment. Langmuir, 15 (13):4321–4323.

Onda, T., Shibuichi, S., Satoh, N., Tsujii, K., 1996. Super-water-repellent fractal surfaces. Langmuir,

12(9), 2125-2127.

Ou, J., Perot, B., Rothstein, J.P., 2004. Laminar drag reduction in microchannels using superhydrophobic surfaces. Physics of Fluids.

Öner, D., McCarthy, T. J., 2000. Ultrahydrophobic surfaces. Effects of topography length scales on wettability. Langmuir, 16(20), 7777-7782.

Patankar, N. A., 2003. On the modeling of hydrophobic contact angles on rough surfaces. Langmuir, 19(4), 1249-1253.

Rothstein, J. P., 2010. Slip on superhydrophobic surfaces. Annual Review of Fluid Mechanics, 42, 89-109.

Shiu, J. Y., Kuo, C. W., Chen, P., Mou, C. Y., 2004. Fabrication of tunable superhydrophobic surfaces by nanosphere lithography. Chemistry of materials, 16(4), 561-564.

Watanabe, K., Yanuar, H., Udagawa, H., 1999. Drag reduction of Newtonian fluid in a circular pipe with highly water-repellent wall. J. Fluid Mech, 381: 225.

Woolford, B., Prince, J., Maynes, D., Webb, B.W., 2009. Particle image velocimetry characterization of turbulent channel flowwith rib patterned superhydrophobic walls, Physics of Fluids, 21(1-8): 085106.

Lu, S., Yao, Z.H., Hao, P.F., Fu, C.S., 2010. Drag reduction in ultrahydrophobic channels with micro-nano structured surfaces. Science China, Physics, Mechanics & Astronomy, 2010.7.

Zhang, J.X., Yao, Z.H., Lu, S., Hao, P.F., Fu, C.S., 2013, Drag reduction in turbulent flows over superhydrophobic surfaces with micro-nano textures, The 14th Asia Congress of Fluid Mechanics, Hanoi and Halong, Vietnam, 0777-0782.